# The metabolic pattern of idiopathic REM sleep behavior disorder reflects early-stage Parkinson's disease

Sanne K. Meles[1]; Remco J. Renken[2]; Annette Janzen[3]; David Vadasz[3]; Marco Pagani[4,5,6]; Dario Arnaldi[7]; Silvia Morbelli[8]; Flavio Nobili[7]; REMPET study group; Geert Mayer[3,9]; Klaus L. Leenders[1*]; Wolfgang H. Oertel[3,10*]        (* shared last authorship)

**The REMPET study group:**

Elisabeth Sittig-Wiegand[3]; Candan Depboylu[3]; Kathrin Reetz[11]; Sebastiaan Overeem[12]; Angelique Pijpers[12]; Fransje E. Reesink[1]; Teus van Laar[1]; Laura K. Teune[1]; Helmut Höffken[13]; Marcus Luster[13]; Lars Timmermann[3], Karl Kesper[14;] Sofie M. Adriaanse[15]; Jan Booij[15;] Gianmario Sambuceti[8], Nicola Girtler[16]; Cathrine Jonsson[17]

[1]Department of Neurology, University of Groningen, University Medical Center Groningen, The Netherlands
[2]Neuroimaging Center, Department of Neuroscience, University of Groningen, The Netherlands
[3]Department of Neurology, Philipps-Universität Marburg, Marburg, Germany
[4]Institutes of Cognitive Sciences and Technologies, CNR, Rome, Italy
[5]Department of Nuclear Medicine, Karolinska Hospital, Stockholm, Sweden
[6]Department of Nuclear Medicine, University of Groningen, University Medical Center Groningen, The Netherlands
[7]Clinical Neurology, Department of Neuroscience (DINOGMI), University of Genoa and IRCCS AOU San Martino-IST, Genoa, Italy
[8]Nuclear Medicine, Department of Health Sciences (DISSAL), University of Genoa and IRCCS AOU San Martino-IST, Genoa, Italy
[9]Hephata Klinik, Schwalmstadt, Germany
[10]Institute for Neurogenomics, Helmholtz Center for Health and Environment, München, Germany
[11]Department of Neurology and JARA-BRAIN Institute Molecular Neuroscience and Neuroimaging, Aachen University, Aachen, Germany
[12]Kempenhaeghe Foundation, Sleep Medicine Centre, Heeze, The Netherlands
[13]Department of Nuclear Medicine, Philipps-Universität Marburg, Marburg, Germany
[14]Department of Internal Medicine, Section Respiratory Diseases, Philipps Universität Marburg, Marburg, Germany
[15] Department of Nuclear Medicine, Academic Medical Center, Amsterdam, The Netherlands
[16]Clinical Psychology, Department of Neuroscience (DINOGMI), University of Genoa and IRCCS AOU San Martino-IST, Genoa, Italy
[17]Medical Radiation Physics and Nuclear Medicine, Imaging and Physiology, Karolinska University Hospital, Stockholm, Sweden

Corresponding author: Sanne K. Meles, MD, Department of Neurology, University Medical Center Groningen.  Hanzeplein 1, PO Box 30.001; 9700 RB Groningen, The Netherlands

Phone: +31 50 361 5615; Fax +31 50 3611707; E-mail address: s.k.meles@umcg.nl

Running head: the metabolic pattern of iRBD (32 characters)

Total word count: 5711 (excluding tables)

Number of words in abstract: 322; Number of words in main text: 3172

Number of figures: 5; Number of tables: 2; supplementary documents: 1 (PDRP scores in PD)

CONFLICT OF INTEREST

FUNDING SOURCES

ABSTRACT

**Rationale:** Idiopathic REM sleep behavior disorder (iRBD) is considered a prodromal stage of Parkinson's disease (PD) and other Lewy-body disorders. Spatial covariance analysis of $[^{18}F]$-Fluorodeoxyglucose Positron Emission Tomography ($^{18}F$-FDG-PET) data has disclosed a specific brain pattern of altered glucose metabolism in PD. In this study, we identify the metabolic pattern underlying iRBD and compare it to the known PD pattern. To understand the relevance of the iRBD pattern to disease progression, we study the expression of the iRBD pattern in *de novo* PD patients.

**Methods**

The iRBD-related pattern was identified in $^{18}F$-FDG-PET scans of 21 patients with polysomnographically-confirmed iRBD and 19 controls using spatial covariance analysis. Expression of the iRBD-related pattern was subsequently computed in $^{18}F$-FDG-PET scans of 44 controls and 38 de novo, treatment-naïve PD patients. Of these 38 PD patients, 24 had probable RBD according to the Mayo Sleep Questionnaire. Neuropsychological evaluation showed mild cognitive impairment in 20 PD patients (PD-MCI), of whom sixteen also had concomitant RBD and roughly half (11/20) had bilateral motor symptoms.

**Results**

The iRBD-related pattern was characterized by relative hypermetabolism in cerebellum, brainstem, thalamus, sensorimotor cortex, and hippocampus, and by relative hypometabolism in middle cingulate, temporal, occipital and parietal cortices. This topography partially overlapped with the PD-related pattern (PDRP). The iRBD-related pattern was significantly expressed in PD patients compared to controls (P<0.0001). iRBD-related pattern expression was not significantly different between PD patients with and without probable RBD, or between PD patients with unilateral or bilateral parkinsonism. iRBD-related pattern expression was higher in PD-MCI patients, compared

to PD patients with preserved cognition (P=0.001). Subject scores on the iRBD-related pattern were highly correlated to subject scores on the PDRP (r=0.94, P<0.0001).

**Conclusion:** In conclusion, our results show that the iRBDRP is an early manifestation of the PDRP. Expression of both PDRP and iRBDRP was higher in patients with a more **severe form of PD** (PD-MCI), which indicates that expression of the two patterns increases with disease severity.

INTRODUCTION

Most patients with idiopathic REM sleep behavior disorder (iRBD) will develop Parkinson's disease (PD) or Dementia with Lewy bodies (DLB) on long-term clinical follow-up  (1, 2, 3, 4, 5, 6). In such patients, RBD indicates the presence of alpha-synuclein pathology in specific brainstem nuclei that regulate REM sleep (7). It is postulated that over time, the pathological process spreads to other brain areas (8). When the substantia nigra is reached, the ensuing degeneration of the presynaptic dopaminergic system causes the typical motor features of the disease, at which point a PD diagnosis can be made (9, 10). Patients with iRBD, by definition, have not yet developed motor symptoms, and provide a unique opportunity to study the early (prodromal) stages of a patient subgroup with alpha-synucleinopathy (9).

The clinical manifestations of PD are caused by functional changes in multiple neuronal networks, reflected by a typical pattern of abnormal glucose utilization in specific brain regions on [$^{18}$F]-Fluorodeoxyglucose Positron Emission Tomography ($^{18}$F-FDG-PET), referred to as the PD-related pattern (PDRP). The PDRP is characterized by relatively increased metabolism in the thalamus, globus pallidus/putamen, cerebellum and pons; and by relative hypometabolism in the occipital, temporal, parietal and frontal cortices. The PDRP has been consistently identified in several PD populations using spatial covariance analysis (i.e. with the Scaled Subprofile Model and Principal Component Analysis (SSM/PCA)) (11, 12, 13, 14, 15, 16, 17, 18). Expression of the PDRP can be quantified in new $^{18}$F-FDG-PET scans (12), which can be used to investigate group differences and relationships with clinical characteristics.

PDRP expression was significantly higher in ^{18}F-FDG-PET scans of patients with iRBD, compared to age-matched controls *(19, 20, 21)*. Moreover, high baseline PDRP subject scores were associated with a higher risk of developing PD in the next five years *(19)*.

Wu *et al* investigated the metabolic topography of iRBD applying SSM/PCA to ^{18}F-FDG-PET data of 21 patients with iRBD and 21 age-matched controls *(20)*. The iRBD-related pattern (iRBDRP) showed partial overlap with the PDRP. Interestingly, iRBDRP expression was high in patients with iRBD and in early-stage PD patients with unilateral parkinsonism (Hoehn and Yahr stage 1), but lower in more advanced PD patients (Hoehn and Yahr stage 2), suggesting that the iRBDRP contains altered metabolism in regions specific to the prodromal or early stages of PD.

PD patients with concomitant RBD are thought to have a rapidly progressive subtype of the disease with a higher risk of subsequent cognitive decline *(22)* underscoring the potential of the iRBDRP to provide insights into the evolution of functional changes in PD from its early stages. In this study, we provide a further identification of the iRBDRP in an independent ^{18}F-FDG-PET dataset of 21 iRBD patients and 19 controls. In addition, we study the relationship between the iRBDRP and disease severity by calculating expression of the newly-identified iRBDRP in 38 carefully characterized, *de novo*, treatment-naïve PD patients. We compare iRBDRP expression not only between H&Y stage 1 and 2, but also between PD patients with and without probable RBD, and between PD patients with mild cognitive impairment (PD-MCI) and those with normal cognition (PD-NC).

METHODS

*Participants – iRBD – Cohort A and Cohort B*

Twenty-one patients with iRBD and nineteen age-matched controls (Cohort A) were used for identification of the iRBDRP. Cohort B, consisting of 9 patients with iRBD and 13 age-matched controls, was used for validation. Clinical data of both cohorts are provided in Table 1. iRBD was confirmed by video-assisted polysomnography *(21)*. Subjects in Cohorts A and B underwent ^{18}F-FDG-PET on a Siemens Biograph mCT-64 PET/CT camera (Siemens, Munich, Germany) as described previously *(21)*.

*Participants – Parkinson's disease*

From a previous study, we included ^{18}F-FDG-PET data from 44 healthy controls and 38 consecutive outpatients with *de novo*, drug-naïve PD (Table 2) *(23)*. The Mayo Sleep Questionnaire (MSQ *(24)*) and a clinical interview by a sleep medicine expert was conducted on each patient. A diagnosis of "probable RBD" was made in 24 patients (PD-RBD+). The remaining 14 PD patients had no signs or symptoms of RBD (PD-RBD–). Based on neuropsychological assessment, 20 PD patients were diagnosed with MCI, and 18 had normal cognition. Furthermore, 23 PD patients had unilateral motor symptoms (H&Y stage 1), and 15 had bilateral symptoms (H&Y stage 2). Disease duration was defined by the number of months patients had motor symptoms prior to the diagnosis.

The study was approved by the local Institutional Review Boards. Voluntary written informed consent was obtained from each subject after verbal and written explanation of the study, in accordance with the Declaration of Helsinki.

*$^{18}$F-FDG-PET data preprocessing*

All images were spatially normalized onto an $^{18}$F-FDG-PET template in Montreal Neurological Institute (MNI) brain space *(25)* using SPM12 software (Wellcome Department of Imaging Neuroscience, Institute of Neurology, London, UK), implemented in MATLAB (version 2012b; MathWorks, Natick, MA).

*iRBDRP identification in Cohort A*

The iRBDRP was identified by applying Scaled Subprofile Model and Principal Component Analysis (SSM/PCA) to the $^{18}$F-FDG-PET data of Cohort A. In brief, after anatomical registration, images were masked to remove out-of-brain voxels, log-transformed, and subject and group means were removed. This resulted in a residual profile for each scan. Principal component analysis (PCA) was applied to these residual profiles in voxel space, and the components explaining the top 50% of the total variance were selected for further analysis. For each subject, a score was calculated on each selected principal component (PC). These scores were entered into a forward stepwise logistic regression analysis. The components that could best discriminate between controls and patients *(26)*, were linearly combined to form one disease-related pattern (the iRBDRP). In this linear combination, each component was weighted by the coefficient resulting from the logistic regression model. All voxel weights in the iRBDRP were overlaid on a T1 MRI template in Montreal Neurological Institute (MNI) space for visualization.

*IRBDRP subject scores in Cohort B*

Anatomically-registered images were masked and log-transformed, and subject and group means were removed to obtain a residual profile for each scan. The mask and group mean were

based on Cohort A in the iRBDRP identification process. The subject score was calculated by multiplying the residual profile of each subject with the pattern *(12)*.

In Cohort B, iRBDRP subject scores in controls and iRBD patients were z-transformed to Cohort A controls (i.e. the reference; n=19). iRBDRP z-scores were compared between Cohort B controls and patients with a Student's T-test. If significant, the iRBDRP was considered valid.

*RBDRP subject scores in de novo PD patients*

To account for differences in data-acquisition, iRBDRP subject scores in the PD cohort were z-transformed to the subject scores of the corresponding 44 controls. For reference, we also calculated subject scores for the PD-related pattern (PDRP *(16, 21)*) in the 44 controls and 38 PD patients. Again, PDRP subject scores were z-transformed with reference to the 44 controls (see supplementary material).

*Stable regions in the iRBDRP*

Voxel weights in SSM/PCA patterns can fluctuate to some degree depending on the specific sample of patients and controls that is used for derivation *(27)*. This is especially relevant in the study of iRBD because it is a heterogeneous patient group. To investigate which regions in the iRBDRP were stable, we performed a bootstrap resampling (1000 repetitions). Voxels that survived a one-sided confidence interval (CI) threshold of 90% (percentile method) after bootstrapping were overlaid on a T1 MRI template. The (stable) regions in the iRBDRP were compared visually to stable regions in the PDRP.

*Statistical analysis*

iRBDRP z-scores were compared between Cohort B controls and iRBD patients with an independent samples t-test. iRBDRP z-scores were also compared across controls, PD-RBD− and PD-RBD+ groups with a one-way analysis of variance (ANOVA). Post-hoc comparisons were Bonferroni corrected. This analysis was repeated for the comparisons H&Y stage 1 versus H&Y stage 2, and PD-NC versus PD-MCI.

In the 44 controls and 38 PD patients, the correlation between iRBDRP and PDRP subject z-scores was tested for significance with a Pearson's r correlation coefficient. In addition, a voxel-wise correlation of the two patterns was performed with a Pearson's r correlation coefficient.

RESULTS

*iRBDRP identification – Cohort A*

After applying SSM/PCA to Cohort A, the first 10 principal components (explaining 49.8% of the variance) were used for further analysis. The iRBDRP was formed by a linear combination of PC4 and 5 (5.5% and 4.1% of variance, respectively), having approximately equal weights. All voxel weights in the iRBDRP contribute to the iRBDRP subject score (Figure 1). Stable regions (90 CI threshold after bootstrap resampling) are shown in Figure 2 and include relative hypermetabolism in cerebellum, brainstem, thalamus, sensorimotor cortex, and left hippocampus/parahippocampal gyrus; and relative hypometabolism in middle cingulate, temporal, occipital, and parietal cortices.

*iRBDRP subject scores in Cohort B iRBD patients and controls*

iRBDRP subject z-scores were significantly different between controls (n=13) and iRBD patients (n=9) from Cohort B (P=0.04, Table 1, Figure 3). iRBDRP subject scores in Cohort B

controls were not significantly different from subject scores in Cohort A controls. iRBDRP subject scores were also not significantly different between the two iRBD groups (P=0.69).

*iRBDRP subject scores in PD patients*

iRBDRP subject z-scores were significantly higher in PD patients compared to controls (P<0.0001). iRBD z-scores were higher in patients with H&Y stage 1 compared to H&Y stage 2 (Figure 4A), although this difference was not significant (P=0.26). iRBD z-scores were also not significantly different between PD-RBD− and PD-RBD+ (Figure 4C). However, iRBDRP z-scores were significantly higher in PD-MCI patients compared to PD-NC patients (Figure 4B). Compared to the PD-NC group, the PD-MCI group was older, contained a larger proportion of patients with concomitant probable RBD, and a larger proportion of patients with bilateral parkinsonism (Table 2).

*Comparison with the PD-related pattern*

PDRP z-scores were also compared between the different PD subgroups and showed similar trends as the iRBDRP. Specifically, PDRP expression was not significantly different between PD-RBD- and PD-RBD+ (P=1.00), but was significantly different between H&Y stage 1 and H&Y stage 2 PD patients (P=0.024) and between PD-NC and PD-MCI (P=0.004) (see supplementary material for more details). Both PDRP and iRBDRP subject z-scores correlated significantly to age in PD patients (r=0.50; P<0.005), but not in controls (r=0.30; P>0.05). Both PDRP and iRBDRP subject scores were not significantly correlated to disease duration in PD patients (r≈0.02, P>0.80).

Subjects' iRBDRP and PDRP z-scores were highly correlated (r=0.94; P<0.0001; controls and PD patients combined). In addition, voxel weights of the PDRP were correlated to the iRBDRP

(r=0.52). For reference, voxel weights of two PDRPs from independent populations (the PDRP used in this study *(16)* versus the original North-American PDRP published by Eidelberg and colleagues *(14)*) have a stronger voxel-wise correlation (r=0.75).

Stable regions (i.e. those surviving the 90% CI threshold) in both the PDRP and the iRBDRP were overlaid on a T1 template. Figure 5A shows the relatively hypermetabolic stable regions of both patterns. Cerebellum, brainstem, thalamus, and sensorimotor cortex were hypermetabolic in both patterns. In contrast to the PDRP, putamen and pallidum did not show stable involvement in the iRBDRP. Stable hypometabolic regions (Figure 5B) in the two patterns overlapped in parietal, temporal, and occipital cortices.

DISCUSSION

We report the second identification of the iRBDRP in an independent cohort of iRBD patients. The iRBDRP identified in this study disclosed a symmetrical topography, which was strikingly similar to the PDRP. Both patterns are characterized by relatively increased metabolism in cerebellum, brainstem, and thalamus, and by decreased metabolism in occipital, temporal, and parietal cortices. Furthermore, iRBDRP and PDRP subject scores were highly correlated, and both patterns were significantly expressed in *de novo* PD patients compared to controls.

In contrast to the original iRBDRP study by Wu *et al (20)*, we report slightly higher (non-significant) iRBDRP z-scores in patients with bilateral parkinsonism (H&Y2) compared to patients with unilateral parkinsonism (H&Y1). Wu *et al* found significantly lower iRBDRP z-scores in H&Y2 compared to H&Y1 PD patients, and hypothesized that "the iRBDRP is perhaps relevant only for prodromal iRBD cases and likely breaks down with disease progression" *(20)*. This "original" iRBDRP *(20)* was not as similar to the PDRP as our iRBDRP. For instance, the correlation

coefficient between subject scores for the iRBDRP and the PDRP reported in that study (20) was r=0.39, compared to r=0.94 in the current study. Considering that our iRBDRP and PDRP showed considerable overlap, subject scores on the two patterns were highly correlated, and that PDRP expression in iRBD is associated with a higher risk of conversion to PD *(19)*, we hypothesize that the iRBDRP represents an early PDRP pattern. In other words, we suggest that the PDRP and iRBDRP are part of the same spectrum and are both likely to increase with disease progression.

Interestingly, iRBDRP expression was not significantly higher in PD patients with probable RBD compared to PD patients without RBD, suggesting that the iRBDRP is not strictly related to the presence of RBD in PD. In addition, both PDRP and iRBDRP expression were higher in PD-MCI compared to PD-NC. The PD-MCI group was older, contained a larger proportion of patients with bilateral parkinsonism, and the majority had probable RBD. This combination of features may signal a rapidly progressive subtype of PD *(22, 28)*. The fact that such more severely-affected PD patients have higher subject scores on both the PDRP and iRBDRP again suggests that both patterns are markers of severity of the same disease process.

However, some important differences between the iRBDRP and the PDRP were found. The PDRP is characterized by relative hypermetabolism of putamen and pallidum. Although putamen and pallidum were relatively hypermetabolic in the unthresholded iRBDRP, they did not survive our pre-defined threshold (bootstrap resampling), which indicates that these regions were not involved in each iRBD patient. Relatively increased putaminal metabolism is thought to be a functional response to loss of dopaminergic input beyond a certain threshold, and is related to the onset of motor symptoms *(29)*. In a previous study, we showed that 9 of our 21 iRBD patients (Cohort A) had significant loss of dopamine transporter-binding *(21)*, indicating neurodegeneration of the presynaptic

dopaminergic system *(30, 31)*. These nine patients may have contributed to the relative hypermetabolism of putamen/pallidum in the unthresholded iRBDRP.

Furthermore, iRBDRP disclosed relative hypermetabolism of the dorsal aspect of the pons. Pontine hypermetabolism was more extensive in the PDRP. Nuclei that regulate REM sleep circuitry are located in the dorsal pons *(32)* and lie in close proximity to the noradrenergic locus coeruleus (LC), cholinergic pedunculopontine nucleus (PPN), and serotonergic raphe nuclei. Although the spatial resolution of FDG-PET images is not sufficient to discriminate between brainstem nuclei, we note that the clusters in the pons and mesencephalon (Figure 2) overlap with the median raphe *(33)*, LC *(34)*, and partially with the PPN *(35, 36)*. These nuclei are affected early on in PD, prior to degeneration of the dopaminergic system *(8)*. All three systems project to cerebellum and thalamus *(37, 38, 39)*. The PPN additionally projects to the basal ganglia and motor cortex *(37)*, the LC projects to the hippocampus and cortex *(38)*, and the median raphe projects to the hippocampus and cingulate *(39)*. All these regions were identified in the iRBDRP and PDRP. Although the underlying mechanism of relative pontine hyperactivity is unclear, it appears to be a consistent feature of iRBD *(19, 20, 40)* and PD *(11, 12, 13, 14, 15, 16, 17, 18)*.

Relative hippocampal hypermetabolism, another consistent finding in functional imaging studies in iRBD *(20, 41, 42, 43)*, reliably contributed to the iRBDRP, but not to the PDRP. Relative hyper-perfusion of the hippocampus was associated with subsequent development of PD/DLB (n=10) in a 3-year clinical follow-up study of 20 iRBD patients *(40)*. Hypometabolism of the middle cingulate, associated with cognitive decline in longitudinal PD studies *(44, 45, 46, 47)*, appears to be a distinct feature of the iRBDRP, as it was not seen in the PDRP.

Both the "original" *(20)* and current iRBDRP included relative hypermetabolism of the thalamus, hippocampus, and pons; and relative hypometabolism of the temporal and occipital

cortices. However, there are clear differences. Firstly, in contrast to the "original" iRBDRP, our pattern included relative hypermetabolism of cerebellum, putamen, and pallidum, in keeping with Holtbernd *et al (19)*. The two latter regions were not considered stable in our analysis, but did contribute to iRBDRP subject scores. Secondly, Wu *et al* described relatively increased metabolism of middle cingulate, whereas our iRBDRP discloses relatively decreased metabolism of the same region. Thirdly, relative hypometabolism of the parietal cortex appears to be a more salient feature in the current iRBDRP, whereas the occipital cortex was more prominent in the "original" iRBDRP.

It is conceivable that the differences between the two iRBDRPs were caused by heterogeneity in the respective iRBD samples. Although the iRBD cohorts in both studies had similar ages and symptom durations, it is unknown which proportion of patients will develop DLB or PD, and at what time-interval. For example, it is possible that a larger proportion of prodromal DLB patients in the study by Wu *et al* has caused the salient reductions in the occipital cortex. In addition, iRBD patients occasionally develop multiple system atrophy (MSA) instead of PD or DLB *(1, 2, 3, 4, 5, 6)*. MSA is characterized by a very different metabolic pattern *(17)* and could therefore have influenced pattern topography and subject scores.

Furthermore, the iRBDRP in our study was formed by a combination of principal components 4 and 5 (together accounting for 9.6% of the total variance), whereas most disease-related patterns (such as the PDRP) are found amongst the first few PCs (i.e. PC1 and PC2 combined *(16)*, or PC1 in isolation *(14, 18)*). Wu *et al* also identified their iRBDRP by principal component 1 (14% of the variance) *(20)*. The fact that the current iRBDRP was found amongst components with lower eigenvalues, indicates that the between-subject variance was larger than the between-group variance in the iRBDRP identification cohort (Cohort A: iRBD versus controls). We also evaluated components 1 and 2 in Cohort A. These components did not discriminate significantly between

controls and iRBD patients in Cohort A and Cohort B, and were also not significantly different between PD patients and healthy controls (P>0.05). PC1 and PC2 were similar to the first 2 components which were reported in several cohorts of healthy controls *(48)*. This is perhaps not surprising, as we contrasted controls to patients who did not have parkinsonism, of which the majority (n=12) had normal dopamine transporter scans. The disease-related alterations are weak; a proportion of patients may have a metabolic brain profile which is close to normal. As a consequence, the first few principal components in this dataset describe normal resting-state brain function.

In conclusion, our results suggest that the iRBDRP is an early manifestation of the PDRP. Expression of both PDRP and iRBDRP was higher in patients with **a more severe form of PD** (PD-MCI), which may indicate that expression of the two patterns increases with disease severity. This finding may be relevant for future progression and therapeutic studies in prodromal PD. Clinical and imaging follow-up of our cohort is ongoing and will provide insights to the changes of the iRBDRP over time and in relation to phenoconversion to PD or DLB.

## References

1. Postuma RB, Gagnon JF, Vendette M, Fantini ML, Massicotte-Marquez J, Montplaisir J. Quantifying the risk of neurodegenerative disease in idiopathic REM sleep behavior disorder. *Neurology*. 2009;72:1296-1300.

2. Postuma RB, Lang AE, Gagnon JF, Pelletier A, Montplaisir JY. How does parkinsonism start? prodromal parkinsonism motor changes in idiopathic REM sleep behaviour disorder. *Brain*. 2012;135:1860-1870.

3. Iranzo A, Tolosa E, Gelpi E, et al. Neurodegenerative disease status and post-mortem pathology in idiopathic rapid-eye-movement sleep behaviour disorder: An observational cohort study. *Lancet Neurol*. 2013;12:443-453.

4. Schenck CH, Boeve BF, Mahowald MW. Delayed emergence of a parkinsonian disorder or dementia in 81% of older men initially diagnosed with idiopathic rapid eye movement sleep behavior disorder: A 16-year update on a previously reported series. *Sleep Med*. 2013;14:744-748.

5. Iranzo A, Fernandez-Arcos A, Tolosa E, et al. Neurodegenerative disorder risk in idiopathic REM sleep behavior disorder: Study in 174 patients. *PLoS One*. 2014;9:e89741.

6. Postuma RB, Iranzo A, Hogl B, et al. Risk factors for neurodegeneration in idiopathic rapid eye movement sleep behavior disorder: A multicenter study. *Ann Neurol*. 2015;77:830-839.

7. Boeve BF. Idiopathic REM sleep behaviour disorder in the development of parkinson's disease. *Lancet Neurol*. 2013;12:469-482.

8. Braak H, Del Tredici K, Rub U, de Vos RA, Jansen Steur EN, Braak E. Staging of brain pathology related to sporadic parkinson's disease. *Neurobiol Aging*. 2003;24:197-211.

9. Berg D, Postuma RB, Adler CH, et al. MDS research criteria for prodromal parkinson's disease. *Mov Disord*. 2015;30:1600-1611.

10. Postuma RB, Berg D, Stern M, et al. MDS clinical diagnostic criteria for parkinson's disease. *Mov Disord*. 2015;30:1591-1601.

11. Eidelberg D. Metabolic brain networks in neurodegenerative disorders: A functional imaging approach. *Trends Neurosci*. 2009;32:548-557.

12. Spetsieris PG, Eidelberg D. Scaled subprofile modeling of resting state imaging data in parkinson's disease: Methodological issues. *Neuroimage*. 2011;54:2899-2914.

13. Eidelberg D, Moeller JR, Dhawan V, et al. The metabolic topography of parkinsonism. *J Cereb Blood Flow Metab*. 1994;14:783-801.

14. Ma Y, Tang C, Spetsieris PG, Dhawan V, Eidelberg D. Abnormal metabolic network activity in parkinson's disease: Test-retest reproducibility. *J Cereb Blood Flow Metab*. 2007;27:597-605.

15. Niethammer M, Eidelberg D. Metabolic brain networks in translational neurology: Concepts and applications. *Ann Neurol*. 2012; 72:635-47.

16. Teune LK, Renken RJ, de Jong BM, et al. Parkinson's disease-related perfusion and glucose metabolic brain patterns identified with PCASL-MRI and FDG-PET imaging. *Neuroimage Clin*. 2014;5:240-244.

17. Teune LK, Renken RJ, Mudali D, et al. Validation of parkinsonian disease-related metabolic brain patterns. *Mov Disord*. 2013;28:547-551.

18. Wu P, Wang J, Peng S, et al. Metabolic brain network in the chinese patients with parkinson's disease based on 18F-FDG PET imaging. *Parkinsonism Relat Disord*. 2013;19:622-627.

19. Holtbernd F, Gagnon JF, Postuma RB, et al. Abnormal metabolic network activity in REM sleep behavior disorder. *Neurology*. 2014;82:620-627.

20. Wu P, Yu H, Peng S, et al. Consistent abnormalities in metabolic network activity in idiopathic rapid eye movement sleep behaviour disorder. *Brain*. 2014;137:3122-3128.

21. Meles SK, Vadasz D, Renken RJ, et al. FDG PET, dopamine transporter SPECT, and olfaction: Combining biomarkers in REM sleep behavior disorder. *Mov Disord*. 2017; 32: 1482-1486.

22. Fereshtehnejad SM, Postuma RB. Subtypes of parkinson's disease: What do they tell us about disease progression? *Curr Neurol Neurosci Rep*. 2017;17:34-017-0738-x.

23. Arnaldi D, Morbelli S, Brugnolo A, et al. Functional neuroimaging and clinical features of drug naive patients with de novo parkinson's disease and probable RBD. *Parkinsonism Relat Disord*. 2016;29:47-53.

24. Boeve BF, Molano JR, Ferman TJ, et al. Validation of the mayo sleep questionnaire to screen for REM sleep behavior disorder in an aging and dementia cohort. *Sleep Med*. 2011;12:445-453.

25. Della Rosa PA, Cerami C, Gallivanone F, et al. A standardized [18F]-FDG-PET template for spatial normalization in statistical parametric mapping of dementia. *Neuroinformatics*. 2014;12:575-593.

26. Akaike H. A new look at the statistical model identification. *IEEE Trans Automat Contr*. 1974:716-23.

27. Habeck C, Foster NL, Perneczky R, et al. Multivariate and univariate neuroimaging biomarkers of alzheimer's disease. *Neuroimage*. 2008;40:1503-1515.

28. Zhu RL, Xie CJ, Hu PP, Wang K. Clinical variations in parkinson's disease patients with or without REM sleep behaviour disorder: A meta-analysis. *Sci Rep*. 2017;7:40779.

29. Tang CC, Poston KL, Dhawan V, Eidelberg D. Abnormalities in metabolic network activity precede the onset of motor symptoms in parkinson's disease. *J Neurosci*. 2010;30:1049-1056.

30. Iranzo A, Lomena F, Stockner H, et al. Decreased striatal dopamine transporter uptake and substantia nigra hyperechogenicity as risk markers of synucleinopathy in patients with idiopathic rapid-eye-movement sleep behaviour disorder: A prospective study [corrected. *Lancet Neurol*. 2010;9:1070-1077.

31. Iranzo A, Valldeoriola F, Lomena F, et al. Serial dopamine transporter imaging of nigrostriatal function in patients with idiopathic rapid-eye-movement sleep behaviour disorder: A prospective study. *Lancet Neurol*. 2011;10:797-805.

32. Peever J, Luppi PH, Montplaisir J. Breakdown in REM sleep circuitry underlies REM sleep behavior disorder. *Trends Neurosci*. 2014;37:279-288.

33. Kranz GS, Hahn A, Savli M, Lanzenberger R. Challenges in the differentiation of midbrain raphe nuclei in neuroimaging research. *Proc Natl Acad Sci U S A*. 2012;109:E2000.

34. Keren NI, Lozar CT, Harris KC, Morgan PS, Eckert MA. In vivo mapping of the human locus coeruleus. *Neuroimage*. 2009;47:1261-1267.

35. Zrinzo L, Zrinzo LV, Tisch S, et al. Stereotactic localization of the human pedunculopontine nucleus: Atlas-based coordinates and validation of a magnetic resonance imaging protocol for direct localization. *Brain*. 2008;131:1588-1598.

36. Janzen J, van 't Ent D, Lemstra AW, Berendse HW, Barkhof F, Foncke EM. The pedunculopontine nucleus is related to visual hallucinations in parkinson's disease: Preliminary results of a voxel-based morphometry study. *J Neurol*. 2012;259:147-154.

37. Benarroch EE. Pedunculopontine nucleus: Functional organization and clinical implications. *Neurology*. 2013;80:1148-1155.

38. Delaville C, Deurwaerdere PD, Benazzouz A. Noradrenaline and parkinson's disease. *Front Syst Neurosci*. 2011;5:31.

39. Huot P, Fox SH. The serotonergic system in motor and non-motor manifestations of parkinson's disease. *Exp Brain Res*. 2013;230:463-476.

40. Dang-Vu TT, Gagnon JF, Vendette M, Soucy JP, Postuma RB, Montplaisir J. Hippocampal perfusion predicts impending neurodegeneration in REM sleep behavior disorder. *Neurology*. 2012;79:2302-2306.

41. Mazza S, Soucy JP, Gravel P, et al. Assessing whole brain perfusion changes in patients with REM sleep behavior disorder. *Neurology*. 2006;67:1618-1622.

42. Vendette M, Gagnon JF, Soucy JP, et al. Brain perfusion and markers of neurodegeneration in rapid eye movement sleep behavior disorder. *Mov Disord*. 2011;26:1717-1724.

43. Ge J, Wu P, Peng S, et al. Assessing cerebral glucose metabolism in patients with idiopathic rapid eye movement sleep behavior disorder. *J Cereb Blood Flow Metab*. 2015;35:2062-2069.

44. Bohnen NI, Koeppe RA, Minoshima S, et al. Cerebral glucose metabolic features of parkinson disease and incident dementia: Longitudinal study. *J Nucl Med*. 2011;52:848-855.

45. Tard C, Demailly F, Delval A, et al. Hypometabolism in posterior and temporal areas of the brain is associated with cognitive decline in parkinson's disease. *J Parkinsons Dis*. 2015;5:569-574.

46. Pappata S, Santangelo G, Aarsland D, et al. Mild cognitive impairment in drug-naive patients with PD is associated with cerebral hypometabolism. *Neurology*. 2011;77:1357-1362.

47. Garcia-Garcia D, Clavero P, Gasca Salas C, et al. Posterior parietooccipital hypometabolism may differentiate mild cognitive impairment from dementia in parkinson's disease. *Eur J Nucl Med Mol Imaging*. 2012;39:1767-1777.

48. Spetsieris PG, Ko JH, Tang CC, et al. Metabolic resting-state brain networks in health and disease. *Proc Natl Acad Sci U S A*. 2015;112:2563-2568.

FIGURE LEGENDS
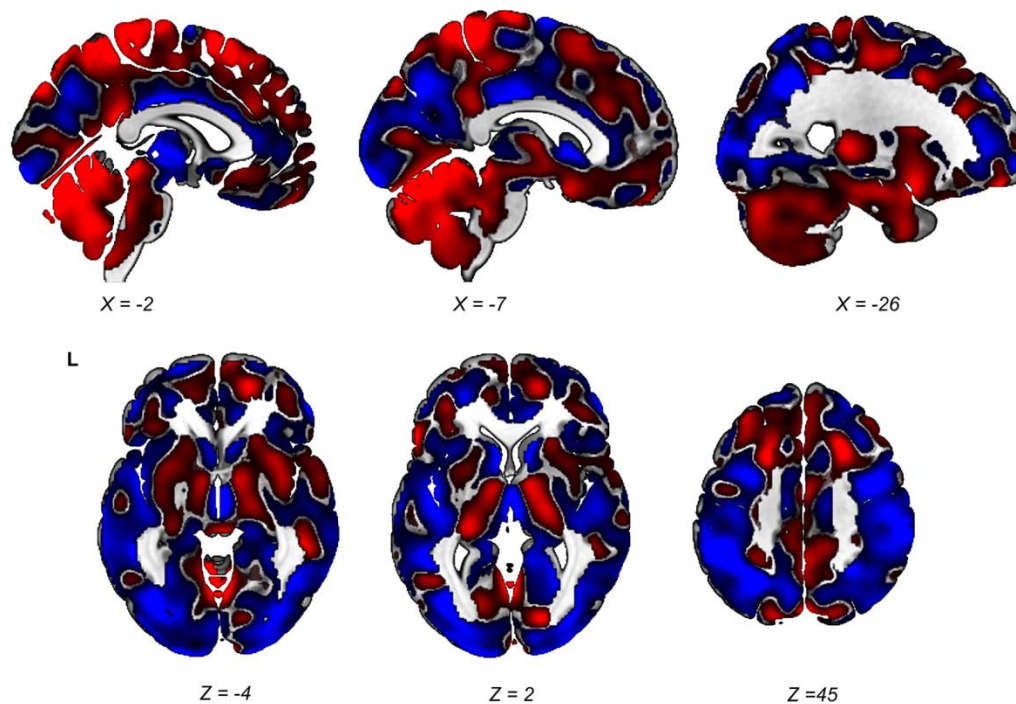


**Figure 1:** The unthresholded iRBDRP overlaid on a T1 MRI template. Red indicates positive voxel weights (relative hypermetabolism) and blue indicates negative voxel weights (relative hypometabolism). L=left. Coordinates in the axial (Z) and sagittal (X) planes are in Montreal Neurological Institute (MNI) standard space.
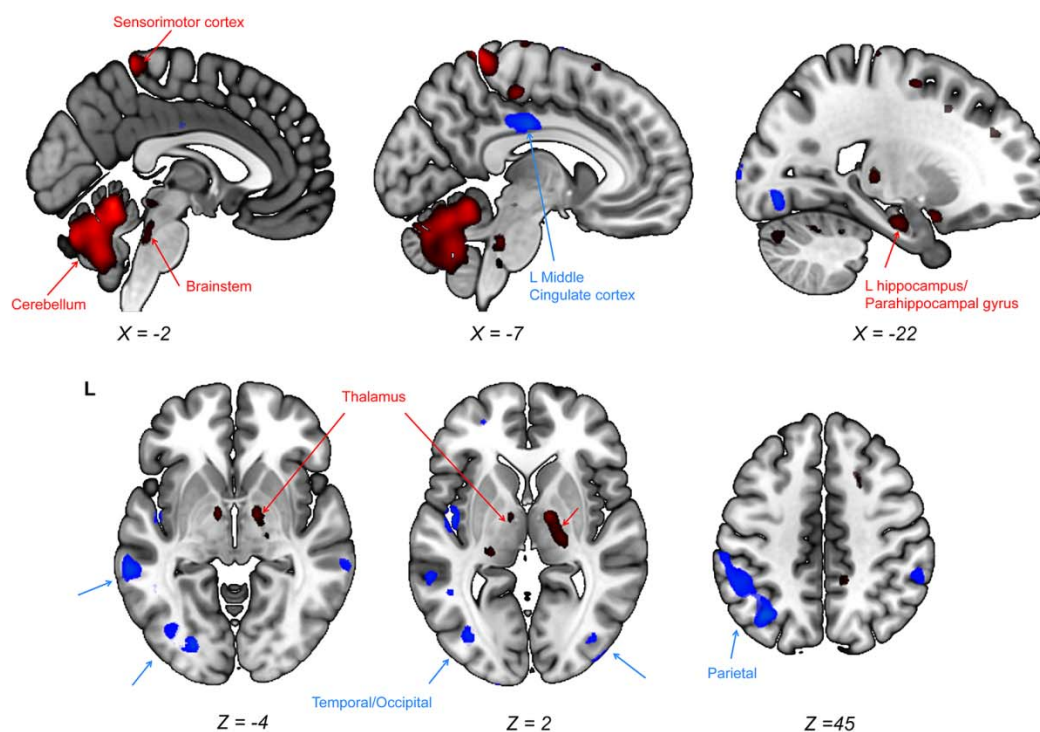
**Figure 2:** Stable voxels (90% confidence interval not straddling zero after bootstrap resampling) of the iRBDRP are visualized by overlaying them on a T1 MRI template. Positive voxel weights are color-coded red (relative hypermetabolism), and negative voxel weights are color-coded blue (relative hypometabolism). L=left. Coordinates in the axial (Z) and sagittal (X) planes are in Montreal Neurological Institute (MNI) standard space.
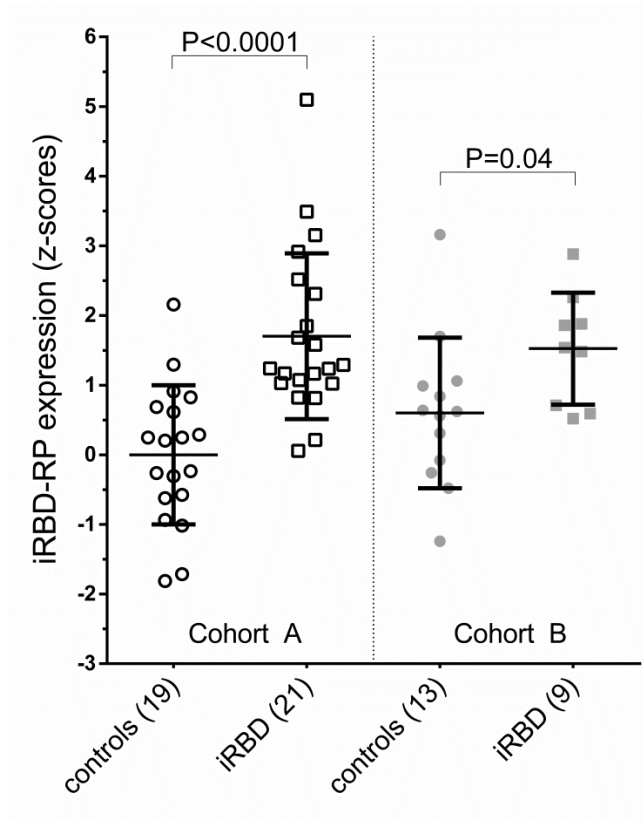
**Figure 3:** iRBDRP subject scores in the derivation cohort (A) and in the validation cohort (B). Subject scores were z-transformed to cohort A controls and compared between groups with a student's t-test.
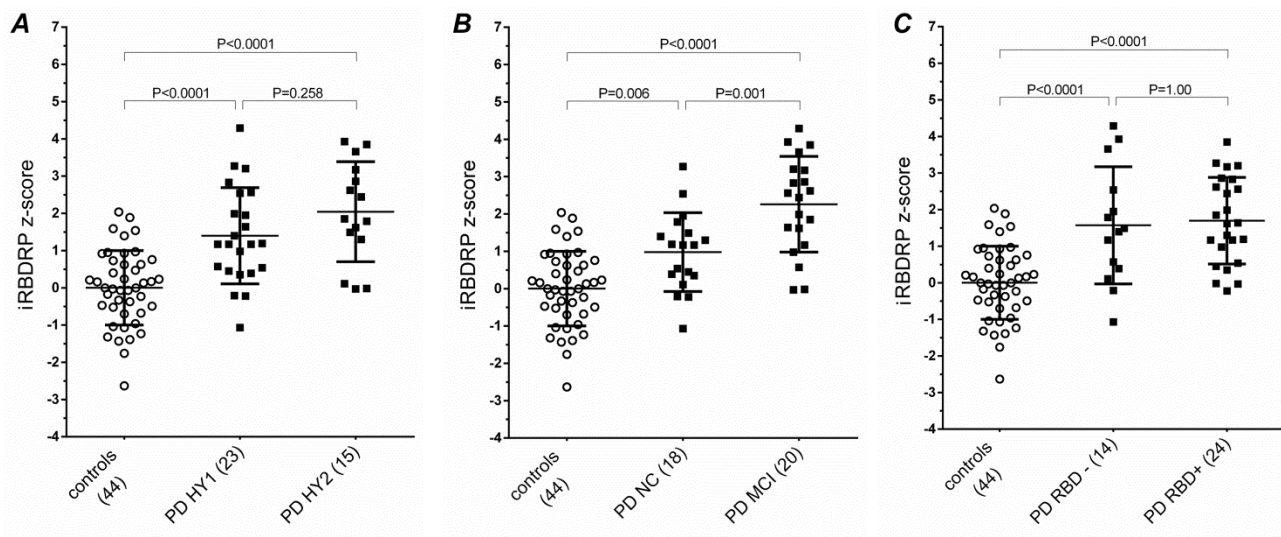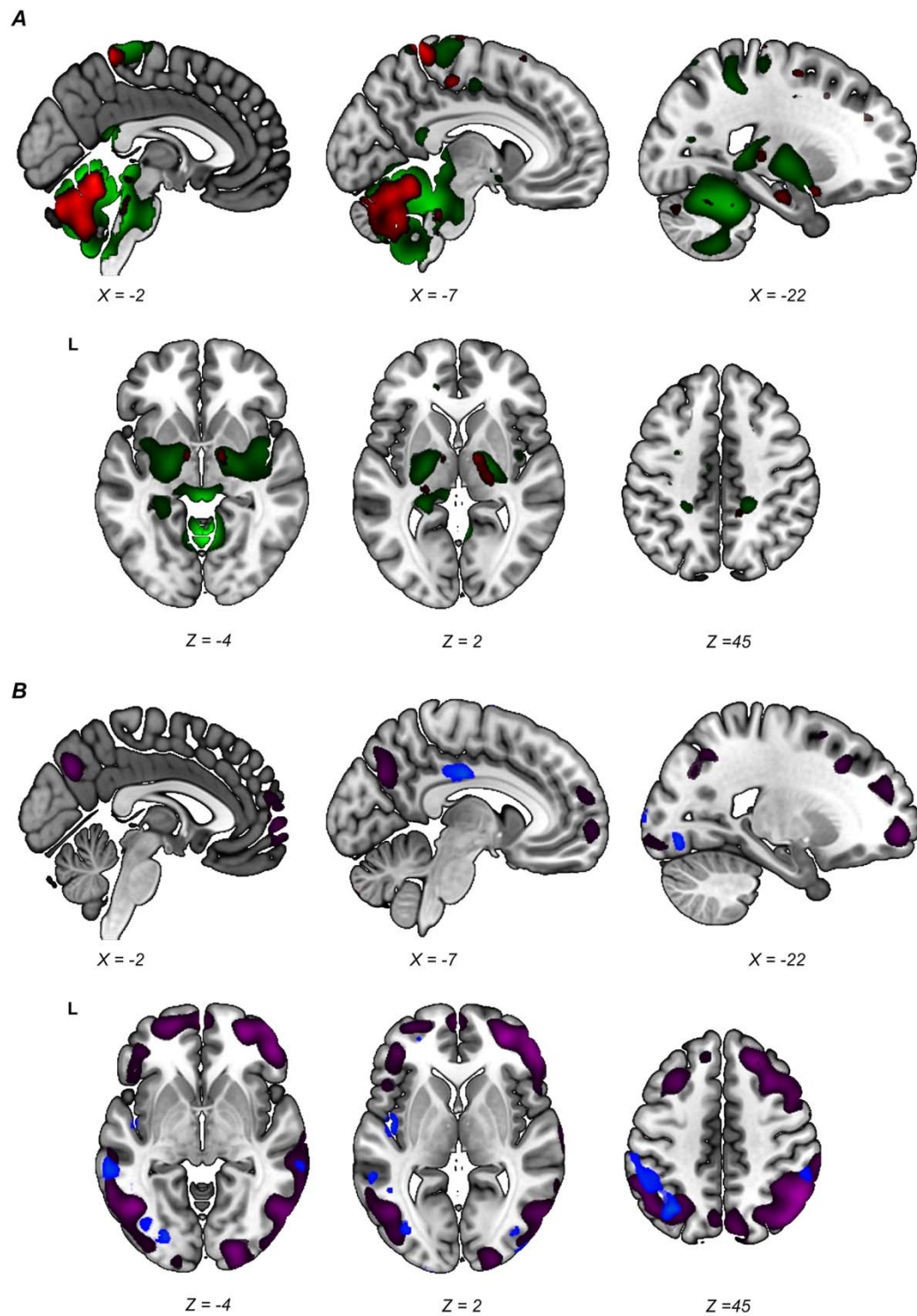
**Figure 4:**

A) IRBDRP subject scores were calculated in controls (n=44), PD patients with Hoehn and Yahr (H&Y) stage 1 (n=23), and PD patients with H&Y stage 2 (n=15). Subject scores were z-transformed with reference to the 44 controls. IRBDRP z-scores were compared across groups with a one-way ANOVA (F(81)=22.4, P<0.0001). IRBDRP z-scores are significantly higher in PD patients compared to controls, but not significantly different between H&Y1 and H&Y2 groups.

B) IRBDRP z-scores were compared across controls, PD patients with normal cognition (PD-NC), and PD patients with mild cognitive impairment (PD-MCI) with a one-way ANOVA (F(81)=30.2, P<0.0001).

C) IRBDRP z-scores were compared across controls, PD patients without RBD (PD-RBD−, n=14) and PD patients with RBD (PD-RBD+, n=24) with a one-way ANOVA (F(81)=20.3, P<0.0001).

P-values in post-hoc group comparisons were Bonferroni-corrected.

**Figure 5** Stable regions in the iRBDRP and PDRP overlap.

Stable voxels (90% confidence interval not straddling zero after bootstrap resampling) of the

iRBDRP and PDRP are overlaid on a T1 MRI template.

A) Stable, relatively hypermetabolic regions of the PDRP (green) and iRBDRP (red).

B) Stable, relatively hypometabolic regions of the PDRP (purple) and iRBDRP (blue).

L=left. Coordinates in the axial (Z) and sagittal (X) planes are in Montreal Neurological Institute

(MNI) standard space.

Table 1: Demographic data of controls and iRBD patients (Cohorts A and B)

| | iRDBRP identification (Cohort A) | | | iRBDRP validation (Cohort B) | | |
|---|---|---|---|---|---|---|
| | Controls | iRBD | P-value* | Controls | iRBD | P-value* |
| N | 19 | 21 | | 13 | 9 | |
| Age (years) [†] | 62.4±7.5 (43-70) | 61.9±5.4 (50-70) | 0.82 | 61.3±8.6 (52-78) | 64.2±6.3 (56-78) | 0.40 |
| Gender (male/female) | 9/10 | 18/3 | 0.010 | 9/4 | 8/1 | 0.36 |
| MoCA | 29 (27-30) | 27 (25.5-28) | 0.003 | 30 (28.5-30)‡ | 28 (27-29) | |
| UPDRS-III | 0 (0-1) | 2 (1-4) | 0.002 | NA | 2 (0-2) | |
| Age at onset RBD [†] | | 55.0±7.1 (37–67) | | | 60.8±6.0 (52–73) | |
| iRBD duration (yrs) | | 6 (3.5-8.0) | | | 4 (1.0-5.0) | |
| iRBDRP z-scores | 0±1 | 1.7±1.2 | <0.0001 | 0.6±1.1 | 1.5±0.8 | 0.04 |

* Controls versus iRBD patients; T-test for age; $Chi^2$ for gender, Mann-Whitney U test for UPDRS and MoCA

Values are median (interquartile range) unless specified by [†], indicating mean ± standard deviation (range).

‡ In B controls, Mini-Mental State Examination (MMSE; maximum of 30 points) was used instead of MoCA.

iRBD = idiopathic REM sleep behavior disorder; MoCA= Montreal Cognitive Assessment; MMSE = Mini-Mental State Examination;

UPDRS-III= part three of the Unified Parkinson's Disease Rating Scale (2003 version); NA=not available

Table 2: Demographic data of PD patients and corresponding controls

| | Controls | PD-NC | PD-MCI | P-value[*] |
|---|---|---|---|---|
| N | 44 | 18 | 20 | |
| Age | 68.8±8.7 | 69.1±7.4 | 73.8±5.7 | 0.032 |
| Gender (n male) | 32 (73%) | 11 (55%) | 14 (70%) | |
| RBD (n) | | 8 (44%) | 16 (80%) | |
| H&Y stage 1 (n) | | 14 (78%) | 9 (45%) | |
| H&Y stage 2 (n) | | 4 (22%) | 11 (55%) | |
| PD symptom duration (months) | | 20.7±14.7 | 16.9±12.9 | 0.398 |
| UPDRS-III | | 12.9±6.1 | 17.2±7.0 | 0.050 |
| MMSE | 29.1±0.9 | 28.7±1.0 | 26.9±2.7 | 0.013 |
| PDRP z-score | 0±1 | 1.29±0.30 | 2.60±1.56 | 0.008 |
| iRBDRP z-score | 0±1 | 0.98±1.1 | 2.26±1.3 | 0.002 |

Values are median (interquartile range), unless otherwise specified. [*]Independent T-test: PD-NC versus PD-MCI

RBD = probable (concomitant) REM sleep behavior disorder according to the Mayo Sleep Questionnaire; H&Y = Hoehn and Yahr stage; UPDRS-III= part three of the Unified Parkinson's Disease Rating Scale; MMSE = Mini-Mental State Examination; PDRP = PD-related pattern; iRBDRP = RBD-related pattern.

**The metabolic pattern of idiopathic REM sleep behavior disorder reflects early-stage**

**Parkinson's disease -** Supplementary material

**Figure 1 – Stable voxels of the Parkinson's disease related pattern (PDRP)**
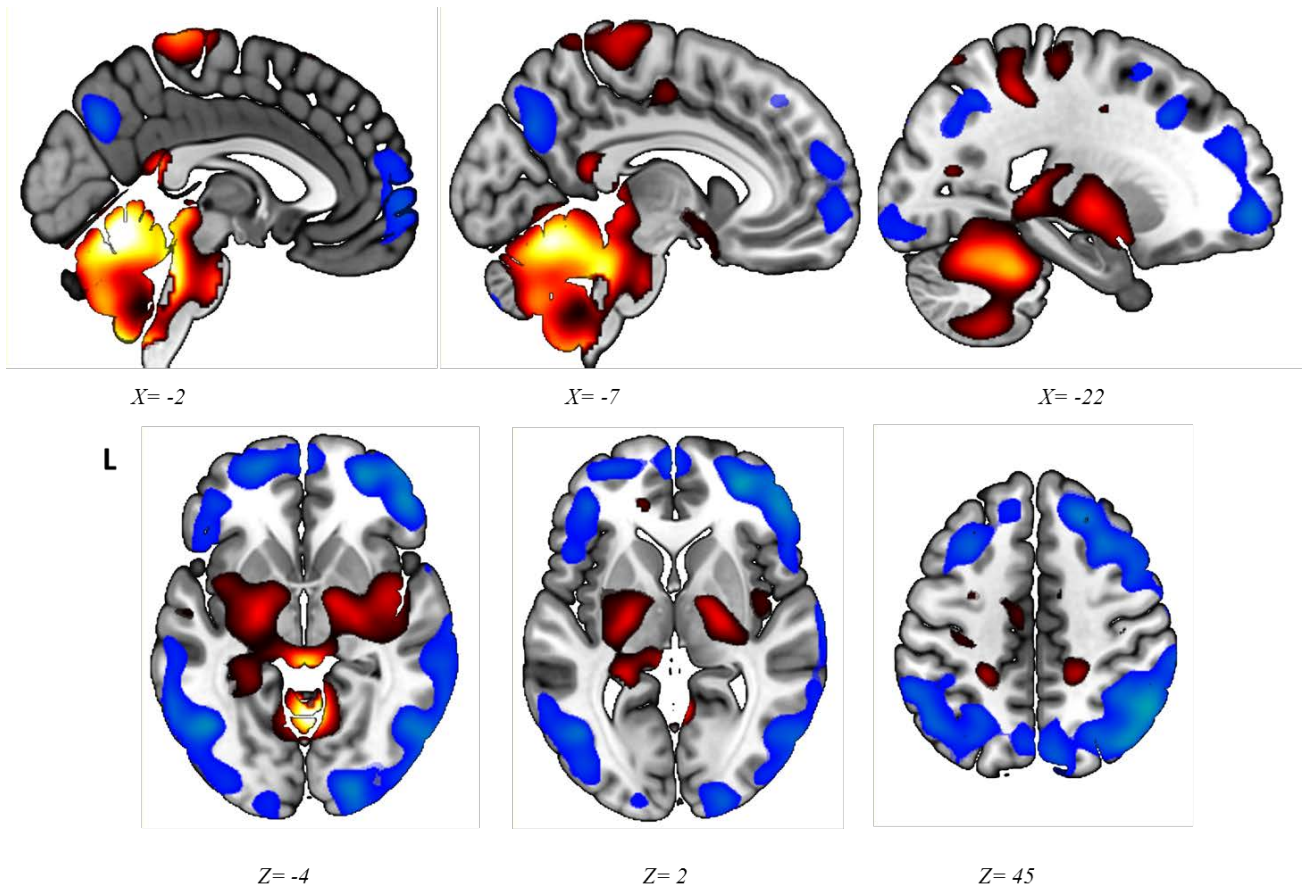


Stable voxels (90% confidence interval not straddling zero after bootstrap resampling) of the PDRP (for detailed description of identification, see: *(1)*) are visualized by overlaying them on a T1 MRI template. Positive voxel weights are color-coded red (relative hypermetabolism) and negative voxel weights are color-coded blue (relative hypometabolism). L=left. Coordinates in the axial (Z) and sagittal (X) planes are in Montreal Neurological Institute (MNI) standard space.

**Figure 2 – Expression of the PDRP across groups**
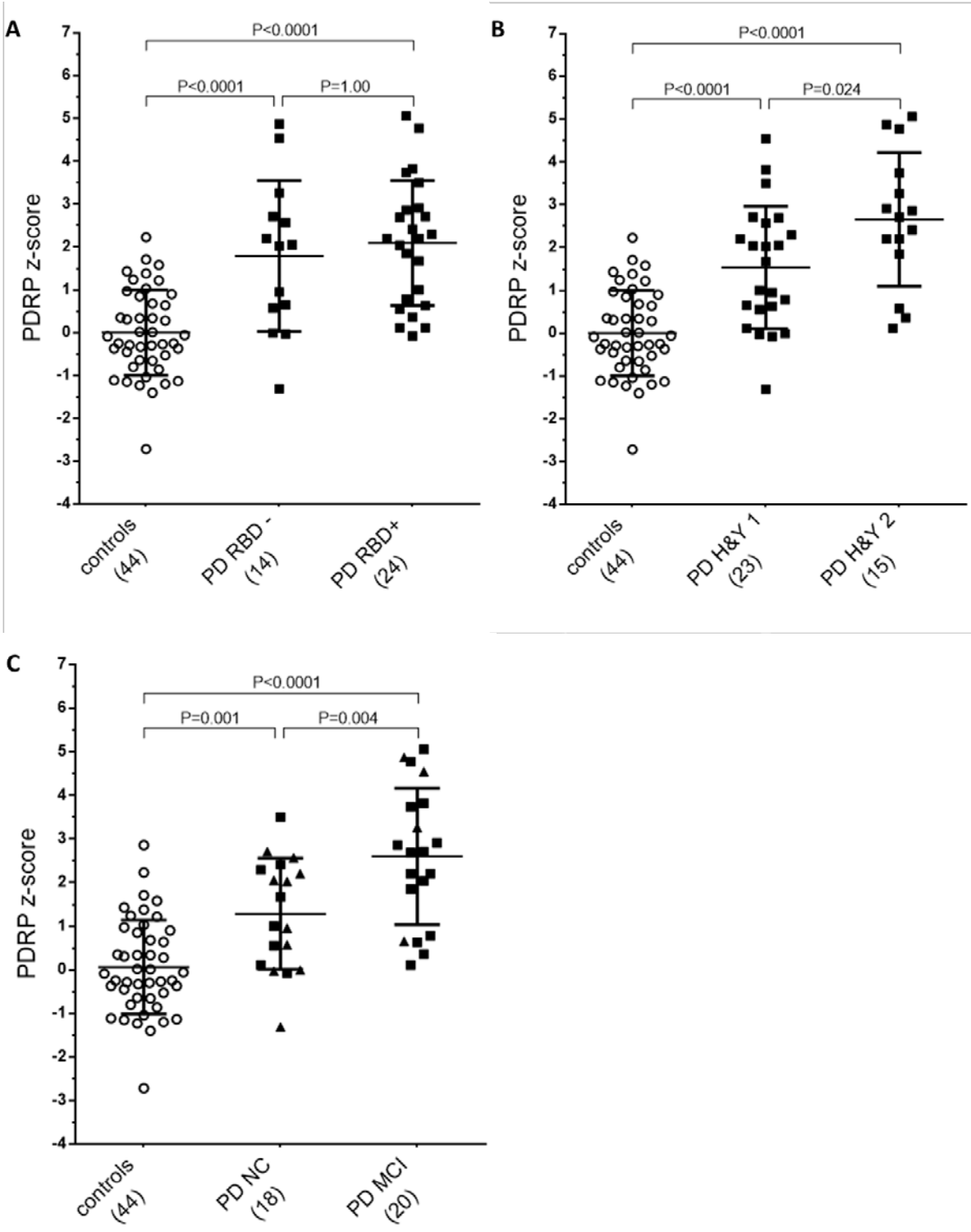
Expression of the PDRP was calculated in 38 *de novo*, treatment-naïve PD patients and 44 corresponding controls (see main text and *(2)* for details). PDRP subject scores were z-transformed to the 44 controls, such that control mean was 0 with a standard deviation of 1.

PDRP z-scores were compared across controls, PD patients without RBD and PD patients with RBD with a one-way ANOVA (F(81)= 24.01; P<0.0001) (Figure 2A). PDRP z-scores were similarly compared across controls, PD patients with unilateral disease (H&Y stage 1), and PD patients with bilateral disease (H&Y stage 2): F(81)= 29.54; P<0.0001 (Figure 2B). Finally, PDRP z-scores were compared across controls, PD patients with normal cognition (PD NC) and PD patients with mild cognitive impairment (PD MCI): F(81)= 32.46; P<0.0001 (Figure 2C). P-values in post-hoc group comparisons were Bonferroni-corrected.

References

1. Teune LK, Renken RJ, de Jong BM, et al. Parkinson's disease-related perfusion and glucose metabolic brain patterns identified with PCASL-MRI and FDG-PET imaging. *Neuroimage Clin*. 2014;5:240-244.

2. Arnaldi D, Morbelli S, Brugnolo A, et al. Functional neuroimaging and clinical features of drug naive patients with de novo parkinson's disease and probable RBD. *Parkinsonism Relat Disord*. 2016;29:47-53.